

## Supplementary file

### **Na<sup>+</sup> doping induced changes in the reduction and charge transport characteristics of Al<sub>2</sub>O<sub>3</sub>-stabilized, CuO-based materials for CO<sub>2</sub> capture**

Qasim Imtiaz<sup>1</sup>, Paula Abdala<sup>1</sup>, Agnieszka Kierzkowska<sup>1</sup>, Wouter van Beek<sup>2</sup>,  
Sebastian Schweiger<sup>3</sup>, Jennifer L. M. Rupp<sup>3</sup> and Christoph Müller<sup>1\*</sup>

<sup>1</sup>Laboratory of Energy Science and Engineering, Department of Mechanical and Process Engineering, ETH Zürich, Leonhardstrasse 27, 8092 Zürich, Switzerland.

<sup>2</sup>Swiss Norwegian Beamlines, European Synchrotron Radiation Facility (ESRF), Grenoble, France.

<sup>3</sup>Electrochemical Materials, Department of Materials, ETH Zürich, Hönggerberggring 64, 8093 Zürich, Switzerland.

\*Corresponding Author

[muelchri@ethz.ch](mailto:muelchri@ethz.ch)

## Experimental set-up for X-ray absorption spectroscopy

A quartz capillary tube with an outer diameter and wall thickness of 1.0 mm and 0.1 mm, respectively, was used as the reactor. In order to optimize the transmission of X-rays and the pressure drop across the capillary cell, each oxygen carrier was mixed with boron nitride (ratio 1:2) and pelletized. The pellets were crushed and sieved in the size range 50 – 100  $\mu\text{m}$ . The oxygen carrier (~2 mg) was fixed in the capillary with two quartz wool plugs and heated under a flow of He to 750  $^{\circ}\text{C}$  using an air blower. The reduction and oxidation reactions were performed using 5 vol. %  $\text{H}_2$  in He and 5 vol. %  $\text{O}_2$  in He, respectively. Gas switching was performed using computer controlled valves. The total gas flow rate for all *in-situ* experiments was 25 mL/min. For both oxygen carriers, XAS measurements were taken in the center of the capillary reactor. A schematic diagram of the experimental setup is shown in [Figure S1](#). The capillary reactor was placed between the first and second ionization chamber that are filled with Ar and  $\text{N}_2$ , respectively. To account for the shift in the absolute energy of the incident X-rays due to the mechanical instability of the monochromator, a copper foil was placed between the second and third chambers to collect a reference spectrum. The off gases were monitored using an on-line mass spectrometer (MS).

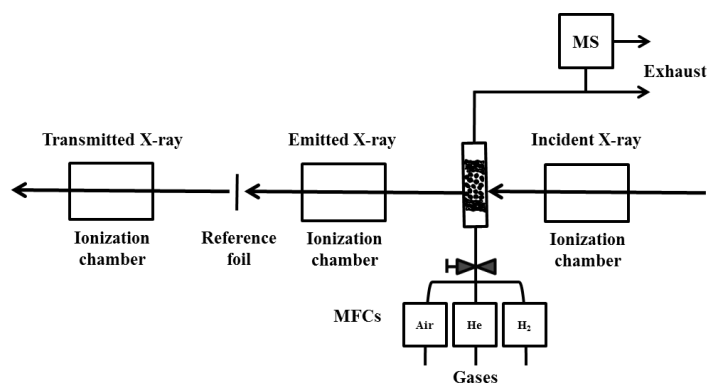


**Figure S1.** Schematic diagram of the experimental set-up used for *in-situ* XAS measurements (MS = mass spectrometer and MFCs = mass flow controllers).

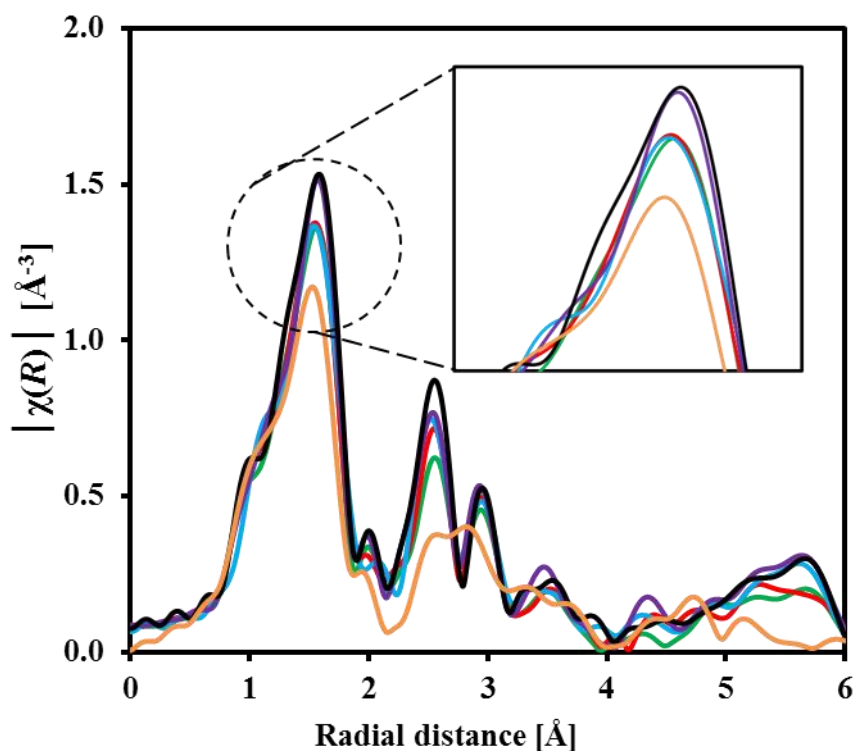


**Figure S2.** Fourier transformed EXAFS functions ( $k^2$ -weighted) of (—) CuAlNa0, (—) CuAlNa1, (—) CuAlNa3, (—) CuAlNa5, (—) CuO and (—) CuAl<sub>2</sub>O<sub>4</sub> measured at the Cu K-edge.

Figure S2 shows that the Fourier transformed EXAFS data of the synthesized oxygen carriers are similar to that of pure CuO with, however, visible differences in the peak heights of the first and second coordination shells of Cu. The first shell around each Cu atom in CuO contains 4 O atoms with a distance between Cu and O atoms of  $\sim 1.95$  Å.<sup>1</sup> On the other hand, CuAl<sub>2</sub>O<sub>4</sub> has a first shell comprising 4 O atoms with a Cu-O distance of  $\sim 1.92$  Å (calculated from the crystallographic data) from the central Cu atom.<sup>2</sup> The structural parameters obtained by fitting the first shell around the central Cu atom in the synthesized oxygen carriers and the references CuO and CuAl<sub>2</sub>O<sub>4</sub> are summarized in Table S1. For the synthesized oxygen carriers, a decrease in the Debye Waller factor and an increase in the Cu-O distance is observed for an increasing Na<sup>+</sup> content. This is due to a decrease in the quantity of CuAl<sub>2</sub>O<sub>4</sub>.

1. S. Asbrink and L. J. Norrby, *Acta Crystall B-Stru*, 1970, B 26, 8-15.

2. H. S. C. O'Neill, M. James, W. A. Dollase and S. A. T. Redfern, *Eur J Mineral*, 2005, 17, 581-586.

**Table S1.** Structural parameters for the first Cu-O shell of the synthesized oxygen carriers and reference materials, as determined by refinement of the theoretical CuO structure.

Material	N <sup>a</sup>	R <sup>b</sup> [Å]	$\sigma^2$ , <sup>c</sup> [Å <sup>2</sup> ]	k-range [Å <sup>-1</sup> ]	R-factor <sup>d</sup> [%]
CuAl <sub>2</sub> O <sub>4</sub>	4.00	1.93 ± 0.01	0.0065 ± 0.0008	3.0 – 13.0	1.010
CuAlNa0	4.00	1.94 ± 0.01	0.0060 ± 0.0009		0.626
CuAlNa1	4.00	1.94 ± 0.01	0.0060 ± 0.0006		0.510
CuAlNa3	4.00	1.94 ± 0.01	0.0061 ± 0.0011		0.880
CuAlNa5	4.00	1.95 ± 0.01	0.0052 ± 0.0006		0.739
CuO	4.00	1.95 ± 0.01	0.0047 ± 0.0004		0.243

<sup>a</sup>N = Cu-O coordination number, fixed; <sup>b</sup>R = Cu-O distance; <sup>c</sup> $\sigma^2$  = EXAFS Debye-Waller factor; <sup>d</sup>R-factor indicates the normalized sum of residuals

The average Cu–O distance obtained for CuO and CuAl<sub>2</sub>O<sub>4</sub> is in agreement with reported crystallographic data.<sup>1-2</sup> From Table S1, it can be seen that the Debye-Waller factor ( $\sigma^2$ ), which is a measure of thermal and structural disorder, of reference CuAl<sub>2</sub>O<sub>4</sub> is higher than that of unsupported CuO. For the synthesized oxygen carriers, the average Cu–O distance in CuAlNa0, CuAlNa1 and CuAlNa3 was determined as ~1.94(1) Å, compared to 1.95(1) Å for CuO. Furthermore, the Debye-Waller factor of CuAlNa0, CuAlNa1 and CuAlNa3 were larger than that of unsupported CuO. In agreement with XRD and XANES measurements (section 3.1), these differences can be attributed to the presence of CuAl<sub>2</sub>O<sub>4</sub> in CuAlNa0, CuAlNa1 and CuAlNa3. In case of CuAlNa5, the average Cu–O distance was 1.95(1) Å, *i.e.* the same as in the CuO reference. However, the Debye-Waller factor of CuAlNa5 was slightly higher than that of pure CuO. The higher Debye-Waller factor may indicate that trace amounts of CuAl<sub>2</sub>O<sub>4</sub> are present in CuAlNa5.

1. S. Åsbrink and L. J. Norrby, *Acta Crystall B*, 1970, B 26, 8-15.

2. H. S. C. O'Neill, M. James, W. A. Dollase and S. A. T. Redfern, *Eur J Mineral*, 2005, 17, 581-586.

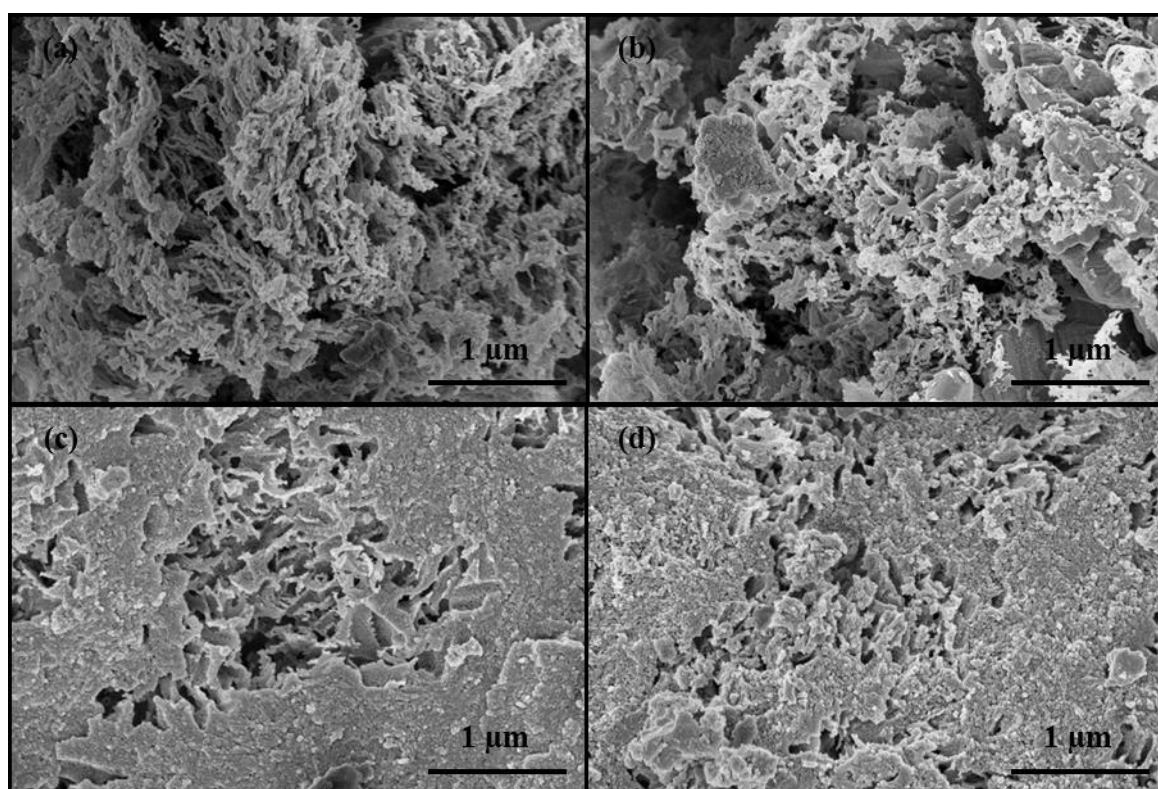


**Figure S3.** High resolution scanning electron micrographs of the oxygen carriers synthesized: (a) CuAlNa0, (b) CuAlNa1, (c) CuAlNa3 and (d) CuAlNa5.

**Table S2.** Surface area and pore volume of the freshly calcined oxygen carriers.

Material	Surface area [m <sup>2</sup> /g]	Pore volume [cm <sup>3</sup> /g]
CuAlNa0	14	0.05
CuAlNa1	20	0.06
CuAlNa3	12	0.04
CuAlNa5	10	0.05

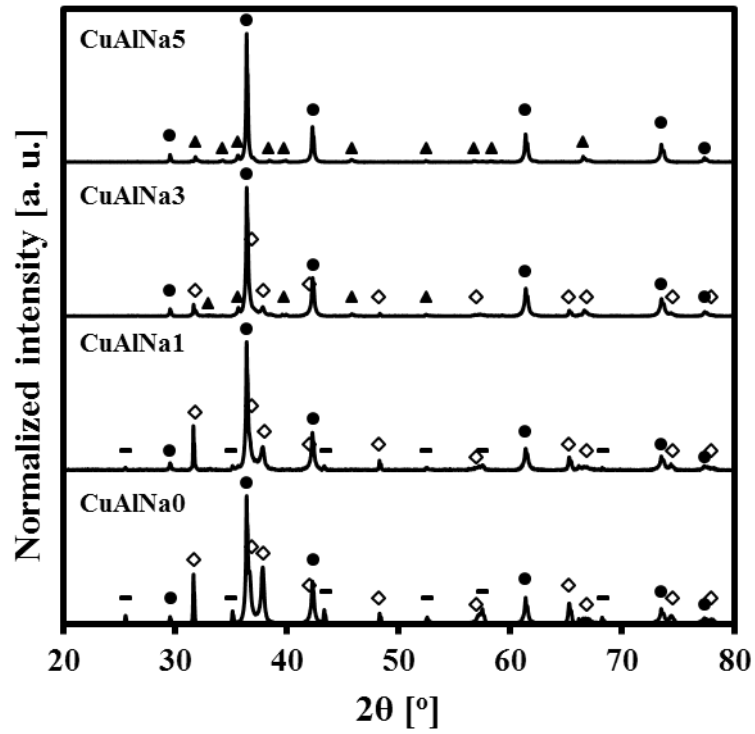


**Figure S4.** X-ray diffractograms of the oxygen carriers reduced in  $N_2$  at  $1150\text{ }^\circ\text{C}$ . The following compounds were identified: (●)  $\text{Cu}_2\text{O}$ , (◇)  $\text{CuAlO}_2$ , (-)  $\text{Al}_2\text{O}_3$  and (▲)  $\text{NaAlO}_2$ .

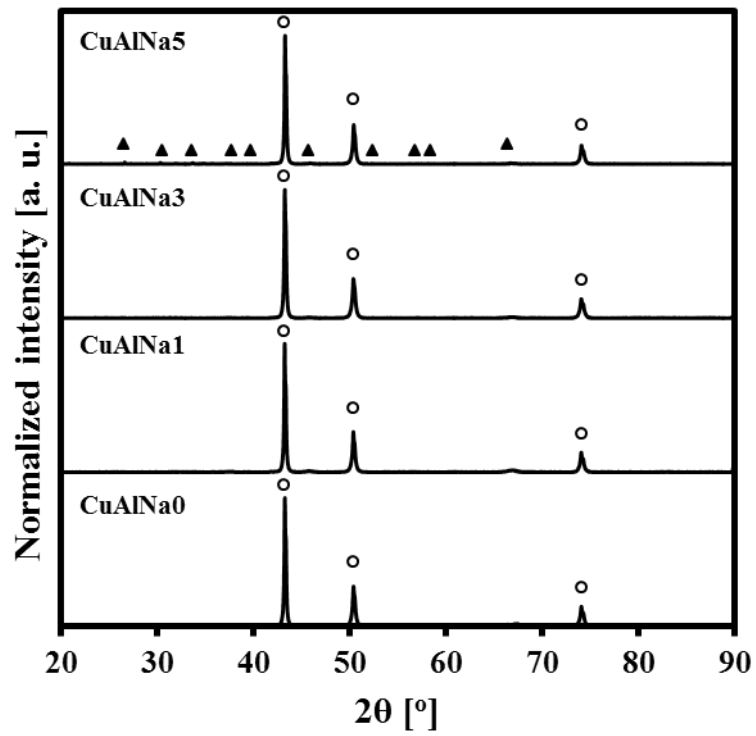


**Figure S5.** X-ray diffractograms of the oxygen carriers reduced using 5 vol. %  $\text{H}_2$  in  $\text{N}_2$  at 1000 °C for 30 min. The following compounds were identified: ( $\circ$ ) Cu and ( $\blacktriangle$ )  $\text{NaAlO}_2$ .

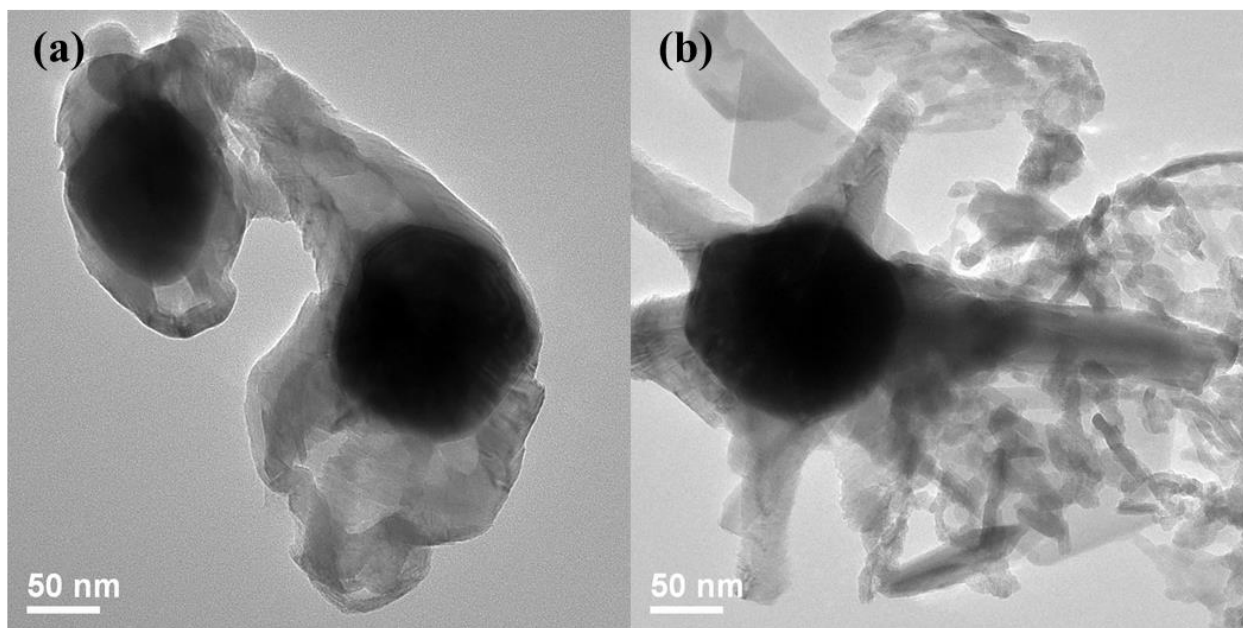


**Figure S6.** Transmission electron micrographs of (a) CuAlNa0 and (b) CuAlNa1 after CH<sub>4</sub>-TPR.



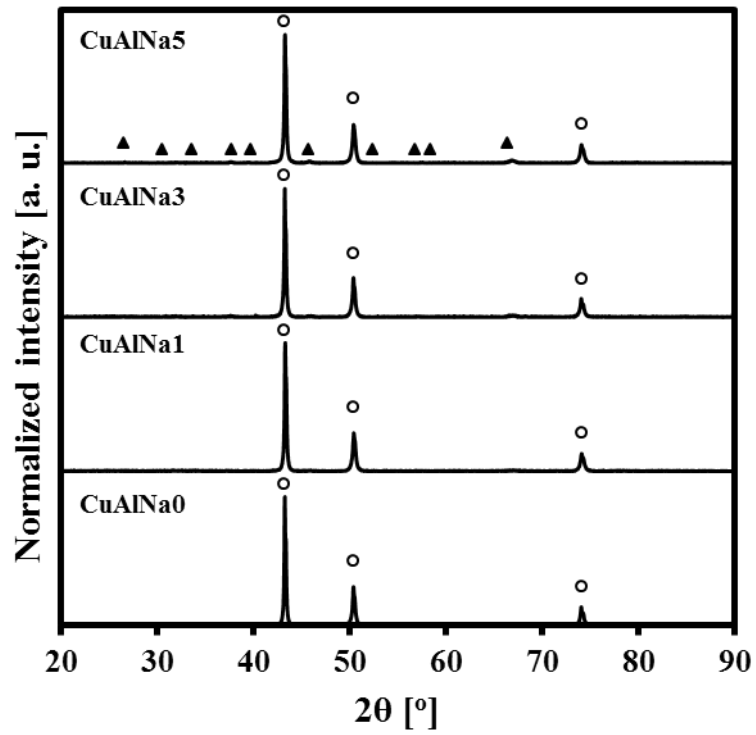


**Figure S7.** X-ray diffractograms of the oxygen carriers reduced using 10 vol. % CH<sub>4</sub> in N<sub>2</sub>. The following compounds were identified: (○) Cu and (▲) NaAlO<sub>2</sub>.

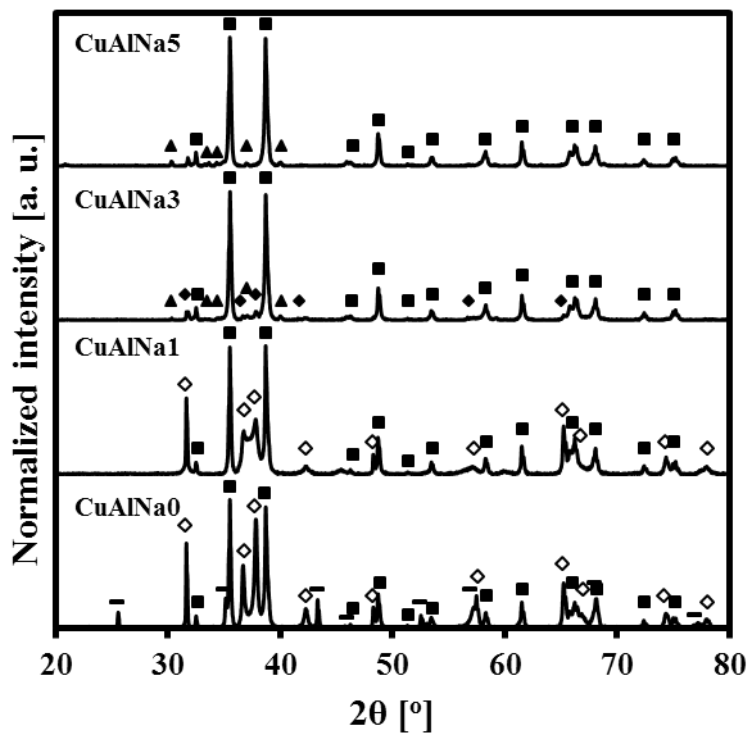


**Figure S8.** X-ray diffractograms of the oxygen carriers cycled under CLOU conditions at 900 °C. The following compounds were identified: (■) CuO, (◆) CuAl<sub>2</sub>O<sub>4</sub>, (◇) CuAlO<sub>2</sub>, (○) Al<sub>2</sub>O<sub>3</sub> and (▲) NaAlO<sub>2</sub>.

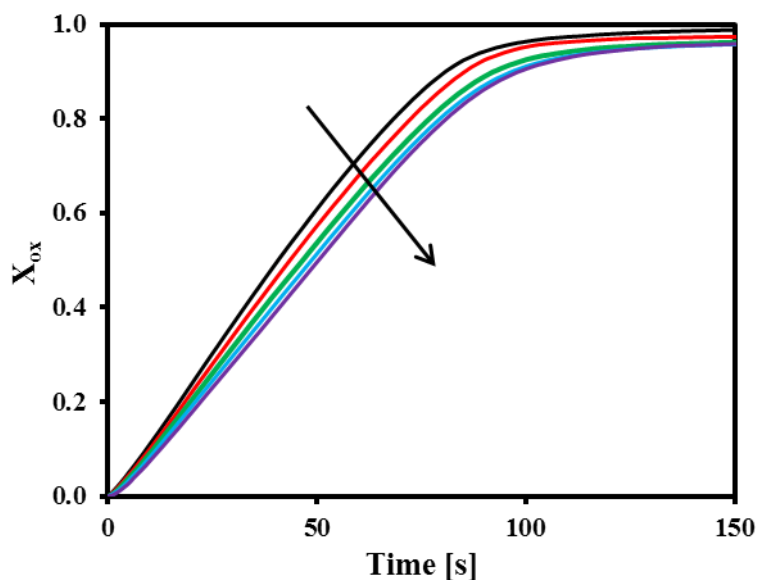


**Figure S9.** Fractional conversion as a function of cycle number during reoxidation of CuAlNa<sub>5</sub> under CLOU conditions at 900 °C: (—) first cycle, (—) second cycle, (—) third cycle, (—) fourth cycle and (—) fifth cycle.

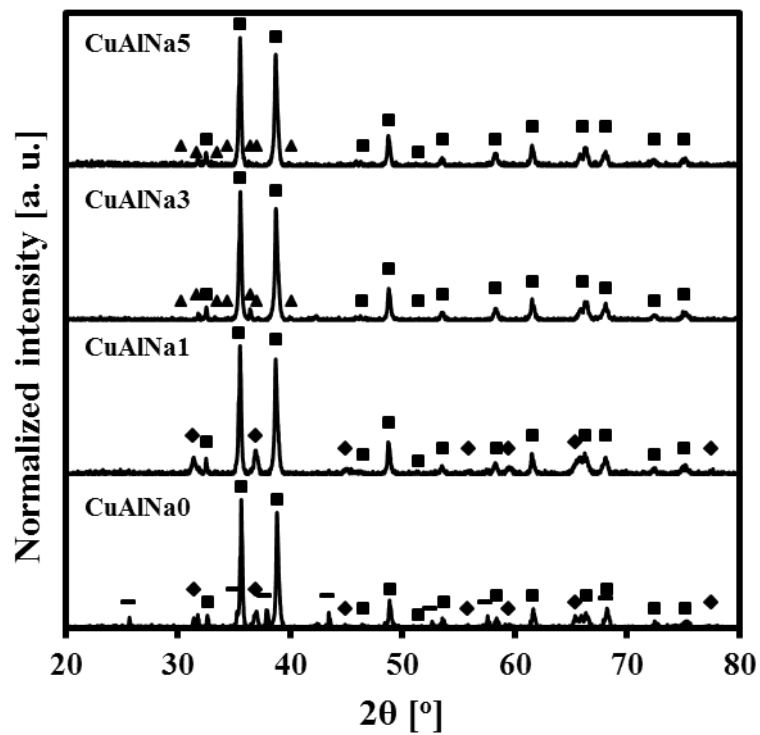


**Figure S10.** X-ray diffractograms of the oxygen carriers cycled 20 times under CLC conditions at 900 °C. The following compounds were identified: (■) CuO, (◆)  $\text{CuAl}_2\text{O}_4$ , (-)  $\text{Al}_2\text{O}_3$  and (▲)  $\text{NaAlO}_2$ .

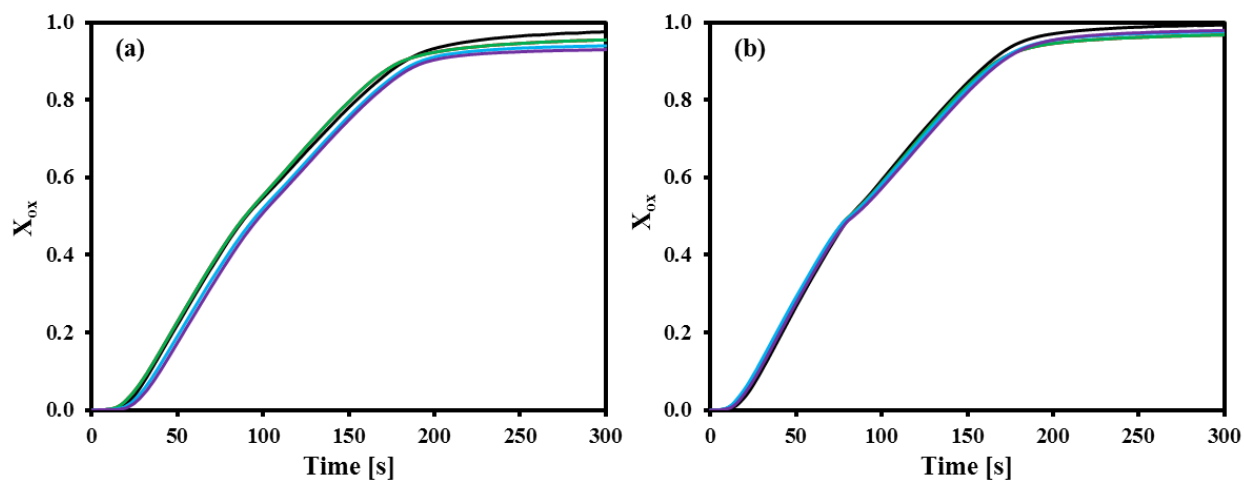


**Figure S11.** Fractional conversion as a function of cycle number during reoxidation of (a) CuAlNa0 and (b) CuAlNa5 under CLC conditions at 900 °C: (—) first cycle, (—) fifth cycle, (—) tenth cycle, (—) fifteenth cycle and (—) twentieth cycle.

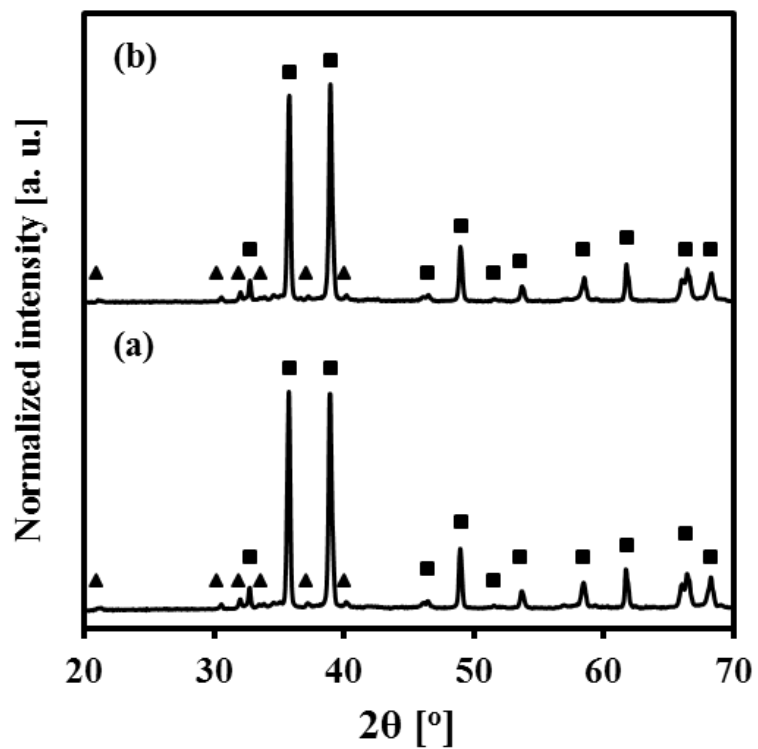


**Figure S12.** X-ray diffractograms of CuAlNa5 (100 cycles, oxidized form): (a) CLC and (b) CLOU conditions at 900 °C. The following compounds were identified: (■) CuO and (▲) NaAlO<sub>2</sub>.

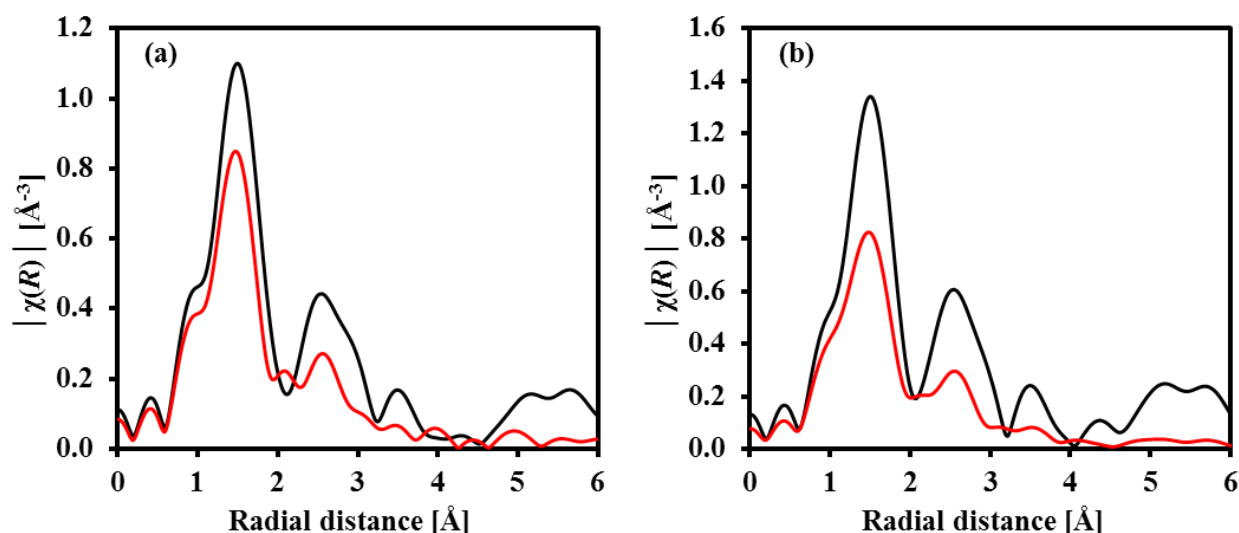


**Figure S13.** Fourier transformed EXAFS functions ( $k^2$ -weighted) of (a) CuAlNa0 and (b) CuAlNa5 measured at the Cu K-edge: (—) 25 °C and (—) 750 °C.

The significant reduction of the amplitude of the Fourier transformed EXAFS functions recorded at 750 °C when compared to room temperature is due to an increase in thermally induced disorder.<sup>3</sup>

**Table S3.** Structural parameters for the first Cu-O shell of CuAlNa0 and CuAlNa5, as determined by refinement of the theoretical CuO structure.

Material	T <sup>a</sup> [°C]	N <sup>b</sup>	R <sup>c</sup> [Å]	$\sigma^{2,d}$ [Å <sup>2</sup> ]	k-range [Å <sup>-1</sup> ]
CuAlNa0	25	4.02 ± 0.46	1.94 ± 0.01	0.0063 ± 0.0017	3.0 – 10.0
CuAlNa0	750	3.26 ± 0.67	1.92 ± 0.02	0.0070 ± 0.0031	
CuAlNa5	25	4.67 ± 0.76	1.94 ± 0.02	0.0056 ± 0.0024	
CuAlNa5	750	3.78 ± 0.68	1.93 ± 0.02	0.0093 ± 0.0029	

<sup>a</sup>T = temperature; <sup>b</sup>N = Cu-O coordination number; <sup>c</sup>R = Cu-O distance; <sup>d</sup> $\sigma^2$  = EXAFS Debye-Waller factor

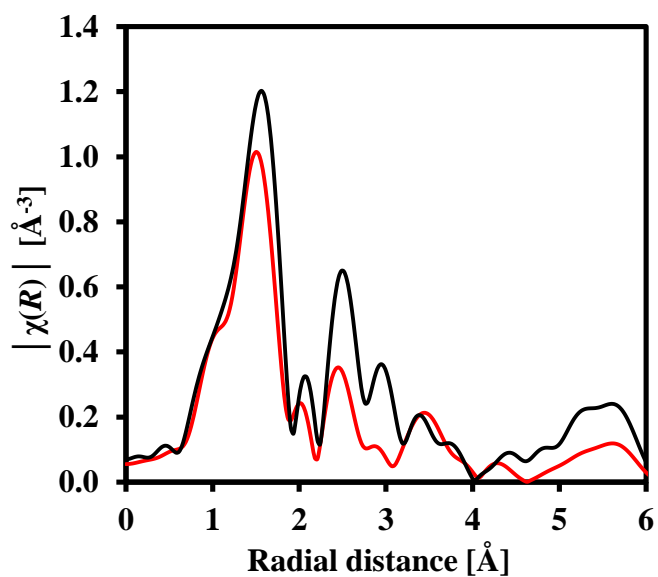


**Figure S14.** Fourier transformed EXAFS functions ( $k^2$ -weighted) of (—) fresh and (—) cycled CuAlNa5 measured at the Cu K-edge at 25 °C.

**Table S4.** Structural parameters for the first (Cu-O) shell of fresh and cycled CuAlNa5, as determined by refinement of the theoretical CuO structure.

Material	$N^a$	$R^b$ [Å]	$\sigma^{2,c}$ [Å <sup>2</sup> ]	k-range [Å <sup>-1</sup> ]
CuAlNa5 (fresh)	$3.60 \pm 0.38$	$1.94 \pm 0.01$	$0.0038 \pm 0.0013$	3.0 – 12.0
CuAlNa5 (cycled)	$3.03 \pm 0.39$	$1.93 \pm 0.01$	$0.0040 \pm 0.0016$	

<sup>a</sup> $N$  = coordination number; <sup>b</sup> $R$  = distance; <sup>c</sup> $\sigma^2$  = EXAFS Debye-Waller factor

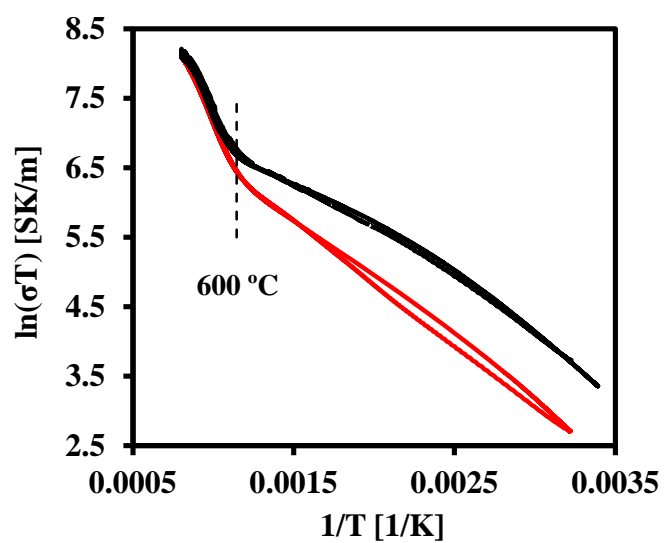


**Figure S15.** Plot of  $\ln(\sigma T)$  as a function of reciprocal temperature for (—) CuAlNa0 and (—) CuAlNa5. The dashed vertical line corresponds to the temperature at which the conductivity regime shifts from intrinsic to extrinsic.